

ELECTROCHEMICAL SENSOR OF MULTIWALLED CARBON NANOTUBE ELECTRODE MODIFIED BY 1-PHENYL-3-METHYL-4-ORTHOFLUORO BENZOYL-5-PYRAZOLONE FOR SENSING DOPAMINE

Emi Norzehan Mohamad Mahbob^{1,2}, Mohamad Syahrizal Ahmad^{1,3*}, Ilyas Md Isa^{1,3*}, Norhayati Hashim^{1,3}, Anwar Ul-Hamid⁴, Mohamad Idris Saidin¹ and Suyanta M. Si⁵

¹Department of Chemistry, Faculty of Science and Mathematics, Universiti Pendidikan Sultan Idris, 35900 Tanjong Malim, Perak Darul Ridzuan, Malaysia

²Faculty of Applied Sciences, Universiti Teknologi MARA, Perak Branch, Tapah Campus, Tapah Road, 35400 Perak Darul Ridzuan, Malaysia

³Nanotechnology Research Centre, Faculty of Science and Mathematics, Universiti Pendidikan Sultan Idris, 35900 Tanjong Malim, Perak Darul Ridzuan, Malaysia

⁴Center for Engineering Research, Research Institute, King Fahd University of Petroleum & Minerals, Dhahran 31261, Saudi Arabia

⁵Department of Chemistry Education, Faculty of Mathematics and Natural Science, Yogyakarta State University, Indonesia

(Received August 26, 2022; Revised March 30, 2023; Accepted April 1, 2023)

ABSTRACT. This work explicates a simple, rapid, and sensitive method for the electrochemical detection of dopamine (DOP) utilising 1-phenyl-3-methyl-4-ortho-fluorobenzoyl-5-pyrazolone (HPMoFBP)/multiwalled carbon nanotube (MWCNT) carbon paste electrode (CPE). The electrochemical behaviour of DOP was performed through cyclic voltammetry and square wave voltammetry. HPMoFBP/MWCNT showed a higher current at the lower potential for the oxidation of DOP compared to bare MWCNT. The sensor's improved electrocatalytic activity was observed to detect in a 1.0×10^{-1} M phosphate buffer saline (PBS) solution at pH 8.0. A good linear regression analysis was observed between electrical response and the concentration of DOP in the range of 1 to 1000 μ M. Under optimized experimental conditions, 1.0×10^{-7} M has been determined as the limit of detection (LOD). The sensor has expressed considerable sensitivity towards DOP detection without interference and is successfully used to determine DOP in dopamine hydrochloride injection.

KEY WORDS: Electrochemical sensor, Dopamine, Pyrazolone, MWCNT, Voltammetry

INTRODUCTION

Numbers of analytical methods such as spectrophotometry, chromatography, chemiluminescence, Fourier transform infrared spectrometry (FTIR), as well as capillary electrophoresis have been extensively used in monitoring drug molecules and targeted compounds that are very important in pharmaceutical analysis and clinical diagnosis [1-5]. Due to high-cost instruments, requirement of skilful experts as well as time consumption for the sample preparation, researchers have shifted their interest in build-up low-cost, simple, rapid, and sensitive electrochemical methods [6]. The easiness between electronic incorporation with electrochemical detection has made the electrochemical detection becomes probable for a varied range of drug molecules which in further allowing wearable sensing [7]. Voltammetric techniques such as square wave voltammetry and cyclic voltammetry are kind of dynamic electroanalytical method used to study the electrochemistry and mechanism of the redox reactions of various inorganic and organic molecules including neurochemicals in bio-fluids such as dopamine [8-10]. In this dynamic electroanalytical method, the concentration of the analyte is obtained from the measurement of

*Corresponding author. E-mail: syahrizal@fsmt.upsi.edu.my ; illyas@fsmt.upsi.edu.my

This work is licensed under the Creative Commons Attribution 4.0 International License

the resulting current. Unlike static electroanalytical method with potentiometric as example, the analyte's concentration is obtained *via* resulting potential [11].

Directly or indirectly participation of dopamine in almost any physiological function including synaptic actions, neuronal handling, and its relation to Parkinson's disease as well as mental health including schizophrenia, Alzheimer's disease, stress, anxiety, and depression has made the dopamine to be one of the most relevant neurotransmitters [12]. According to Masood *et al.* [13], a WHO survey which conducted in August 2020 on mental health over 130 countries exposed that COVID-19 has left an overwhelming impact on the mental health. Even though the mechanisms of anxiety and depression are not fully completely understood, neurotransmitters such as dopamine are involved in the anxiety and depression pathophysiology [14]. Thus, it is significance in quantifying the dopamine concentration in human metabolic fluid since abnormal levels of those neurotransmitters could cause a variety of behavioral, and medical problems [15].

Pyrazolone is a five-membered lactum ring containing two nitrogen and one ketonic group in its structure. Its derivatives show prominent properties in diverse pharmacological, biological, and chemical applications [16]. Considering the promising activity of the pyrazolone derivatives in chemical applications, this study has developed the HPMoFBP/MWCNT paste electrode for the electrochemical detection of dopamine. Cyclic voltammetry (CV) and square wave voltammetry (SWV) for the characterization of the modified CPE will be discussed.

EXPERIMENTAL

Chemicals and reagents

Dopamine hydrochloride (DOP) was acquired from Sigma-Aldrich, USA. Phosphate buffer solution (PBS) was used as a supporting electrolyte. The PBS consists of 1.0×10^{-1} M K_2HPO_4 and 1.0×10^{-1} M KH_2PO_4 (Merck, Germany). The NaOH or diluted HCl was then added to the PBS for adjusting the pH values. Unless otherwise indicated, all reagents were analytical grade without any further purification.

Instrumentation

Electrochemical impedance spectroscopy (EIS) and voltametric analysis were performed using a Galvanostat/Potentiostat model Ref 3000 (Gamry, USA) and a Potentiostat Series-G750 (USA), respectively. Electrochemical measurements were obtained using a standard of three electrode cells with the HPMoFBP or bare MWCNT paste electrodes as a working electrode, a platinum wire as a counter electrode, and an Ag/AgCl electrode MF-2052 (Bioanalytical system, USA) as a reference electrode. The pH of the solution was measured by using Thermo Scientific Orion 2-Star Benchtop pH Meter (USA). Nuclear magnetic resonance spectroscopy was used to get 1H and ^{13}C NMR spectra (NMR, JNM-ECX 500 JEOL, Japan).

Synthesis of 1-phenyl-3-methyl-4-(2-fluorobenzoyl)-5-pyrazolone (HPMoFBP)

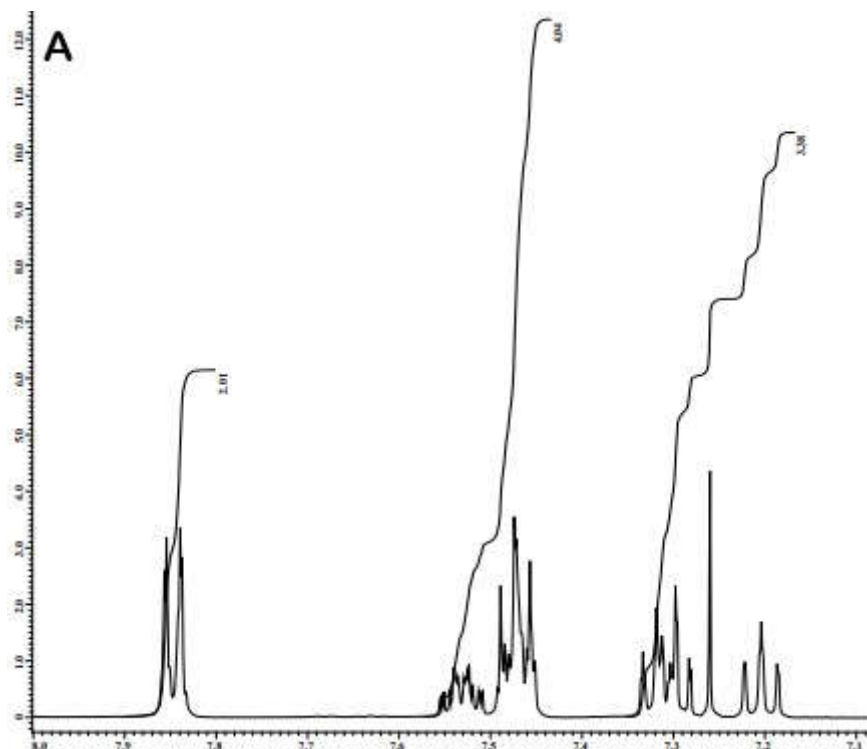
The HPMoFBP compound was prepared using the benzylation process based on a former study with slight modifications [17]. This method used direct benzylation of pyrazolone with benzoyl chloride in the presence of sodium hydroxide. 7.5 g of 1-phenyl-3-methyl-5-pyrazolone (PMP) was weighed and put in a boiling flask. 45 mL of 1,4-dioxane was then added to the PMP before been gentle heated and stirred using a magnetic stirrer till fully dissolution. The 3 M NaOH solution was added, and the mixture was stirred under vigorous stirring for 30 min. 5 mL of 2-fluorobenzoyl chloride was added dropwise to the mixture and refluxed for 1 hour. The reaction mixture was then cooled to room temperature and poured into 75 mL 3 M HCl. The solid phase formed was filtered off, washed with methanol-water, and dried on air.

Electrode fabrication and modification

MWCNTs (95, 90, 85% w/w) and HPMoFBP (5, 10, 15% w/w) were mixed by hand mixing the mixture with 3 drops of paraffin oil and ground carefully using mortar and pestle until the paste was homogenized. Next, the prepared carbon paste was packed firmly into Teflon tube (2 mm in diameter and 5 cm long). One of the ends of the electrode was inserted with copper wire to establish the electrical contact. The other end of the tube was polished by smoothing on a soft paper prior to each measurement. For comparison purpose, the bare MWCNT was prepared using the same procedure but without adding the HPMoFBP.

RESULTS AND DISCUSSION*Characterization of HPMoFBP using nuclear magnetic resonance (NMR) spectroscopy*

The HPMoFBP compound has been characterized using NMR spectroscopy. In the ^1H NMR spectrum (Figure 1A), the peaks present at the range of 7.86 ppm to 7.19 ppm were assigned to the resonance of aromatic structures, such as the phenyl ring and C=O. The ^{13}C NMR spectrum (Figure 1B) exhibited a peak in chemical shift of 188.4 ppm, which assigned to the resonance for C=O and peaks in chemical shift of 160.3 ppm to 116.2 ppm, which assigned to the resonances for aromatic phenyl structures. Moreover, some peaks appeared at chemical shifts of 104.9 ppm, 77.4 ppm, and 14.1 ppm were assigned to the C-F, C-N, and C-H assignments. Hence, it could be concluded that the synthesized compound was HPMoFBP.



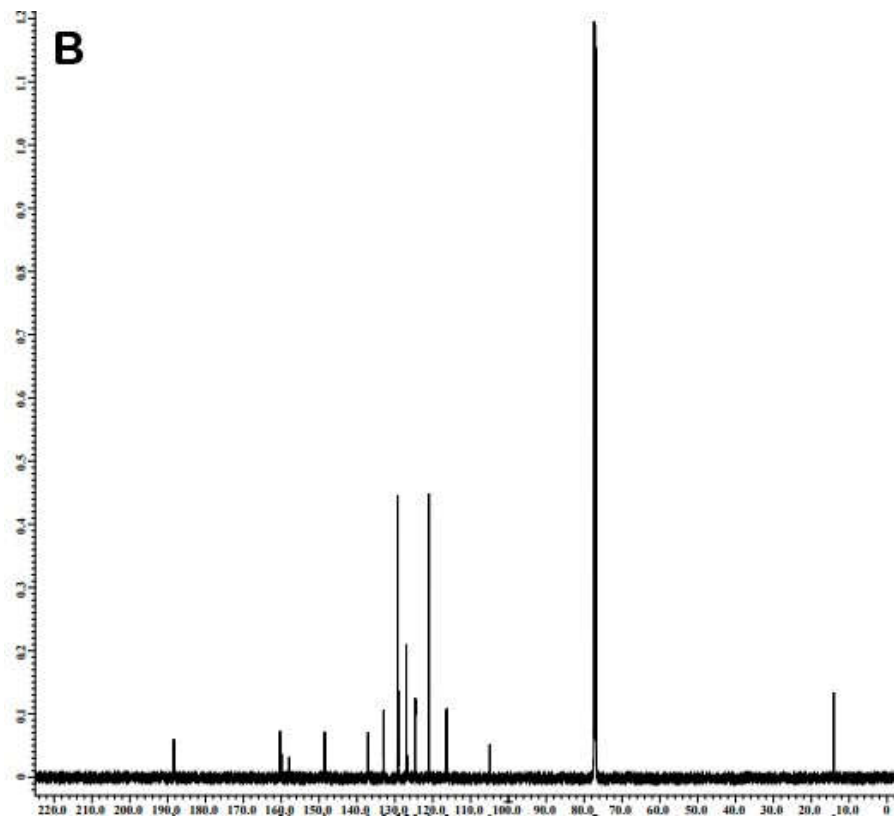


Figure 1. (A) ^1H , and (B) ^{13}C NMR spectra of the HPMoFBP compound.

Electrochemical performance at HPMoFBP/MWCNT paste electrode towards $\text{K}_4[\text{Fe}(\text{CN})_6]$

In order to study the nature of electron transfer of sensing materials, the electroanalytical performance of the HPMoFBP/MWCNT and bare MWCNT were evaluated using cyclic voltammetry (CV) and electrochemical impedance spectroscopy (EIS) towards 4.0×10^{-3} M $\text{K}_4[\text{Fe}(\text{CN})_6]$ containing 1.0×10^{-1} M KCl. 100 mV s^{-1} was used as the scan rate.

The HPMoFBP/MWCNT paste electrode (Figure 2) exhibited redox peak current at $I_{pa} = 6.792 \mu\text{A}$, and $I_{pc} = 5.072 \mu\text{A}$ which is larger oxidation and reduction peaks current compared to the bare MWCNT paste electrode which was $I_{pa} = 5.669 \mu\text{A}$, and $I_{pc} = 1.917 \mu\text{A}$. Moreover, it could be observed that the peak-to-peak separation (ΔE_p) of HPMoFBP/MWCNT decreased to 460.19 mV compared to bare MWCNT with $\Delta E_p = 690.00$ mV. From these findings, it is evident that the introduction of HPMoFBP as an MWCNT modifier is responsible for improving electron transfer rate, electroactive surface area and the conductivity performance of the modified electrode.

The change in electrical resistance of the HPMoFBP/MWCNT and bare MWCNT were evaluated through the EIS-Nyquist plot (Figure 3). Generally, a linear part at lower frequencies represents the diffusion process while a diameter of semicircle impedance response at higher frequencies represents the charge transfer resistance that acts to reduce the flow of electrons at the electrode contact [18]. This study was carried out using a redox probe of 4×10^{-3} M $\text{K}_4[\text{Fe}(\text{CN})_6]$

consisting 1.0×10^{-1} M KCl. As shown in Figure 3, the Nyquist plot of the bare MWCNT displays a larger semicircle (curve a) compared to HPMoFBP/MWCNT (curve b), suggesting lower charge transfer resistance in the interfacial region of HPMoFBP/MWCNT. By fitting the Randle's equivalent electrical circuit system (Figure 3 inset), charge transfer resistance (R_{ct}) values for bare MWCNT and HPMoFBP/MWCNT were 32.31 k Ω and 8.85 k Ω .

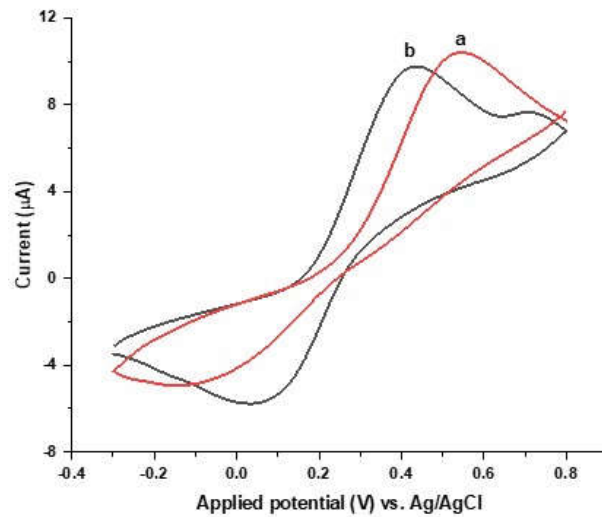


Figure 2. CV of (a) bare MWCNT and (b) HPMoFBP/MWCNT of 4×10^{-3} M $K_4[Fe(CN)_6]$ in 1.0×10^{-1} M KCl, at 100 mV s^{-1} as the scan rate.

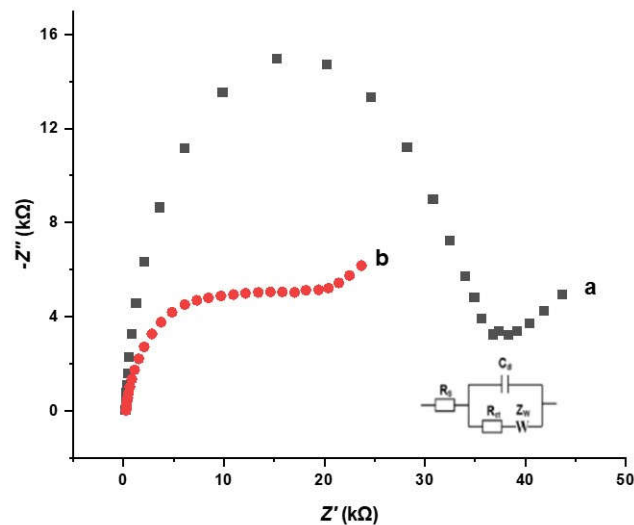


Figure 3. Nyquist plots logged in the solution of 4.0×10^{-3} M $K_4[Fe(CN)_6]$ in 1.0×10^{-1} M KCl utilizing (a) bare MWCNT and (b) HPMoFBP/MWCNT paste electrode. Inset: Randle's equivalent electrical circuit used for data fitting.

In addition, the electron transfer apparent rate constant (k_{apps}) values were calculated for bare MWCNT and HPMoFBP/MWCNT using the Eq. (1).

$$k_{apps} = \frac{RT}{F^2 R_{ct} C} \quad (1)$$

where, R is the gas constant ($8.314 \text{ J mol}^{-1} \text{ K}^{-1}$), T is the absolute temperature (298 K), F is the Faraday's constant (96485 C mol^{-1}) and C is the $\text{K}_4[\text{Fe}(\text{CN})_6]$ solution concentration.

This study found that the calculated values for bare MWCNT and HPMoFBP/MWCNT were 2.06×10^{-6} and $7.52 \times 10^{-6} \text{ cm s}^{-1}$, respectively. The high k_{apps} and low R_{ct} values for HPMoFBP/MWCNT indicating a fast electron transfer process and good conductivity. The EIS results correlated very well with the outcome of CV studies.

The effect of pH

The impact of supporting electrolyte, $1.0 \times 10^{-1} \text{ M}$ PBS pH values in electrochemical determination of $1.0 \times 10^{-4} \text{ M}$ DOP at the HPMoFBP/MWCNT was investigated by SWV due to advantages possessed by SWV such as high speed in analysis, increased analytical sensitivity and relative insensitivity to the presence of dissolved oxygen. As the PBS is more effective in the range between pH 6.2 to 8.0 [22], thus the PBS at pH 6.0, 6.4, 7.0, 7.4, 8.0 and 8.4 have been chosen in evaluating the electrochemical responses of HPMoFBP/MWCNT towards DOP. The DOP oxidation peak current increased with the increment of pH from 6.0 to 8.0, as can be observed in the Figure 4 and then declined with further increment of pH value. Thus, the maximum peak current value at pH 8.0 was selected as the optimum pH for DOP detection in this study.

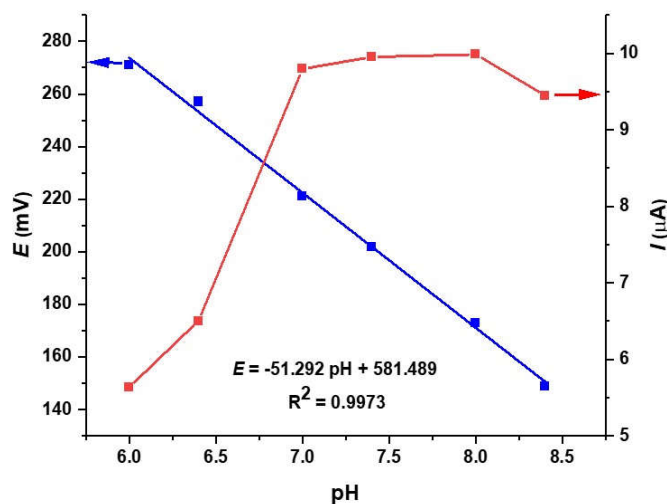


Figure 4. Oxidation peak current (I) and oxidation potential (E) vs. pH plot of $1.0 \times 10^{-1} \text{ M}$ PBS containing $1.0 \times 10^{-4} \text{ M}$ DOP at HPMoFBP/MWCNT paste electrode.

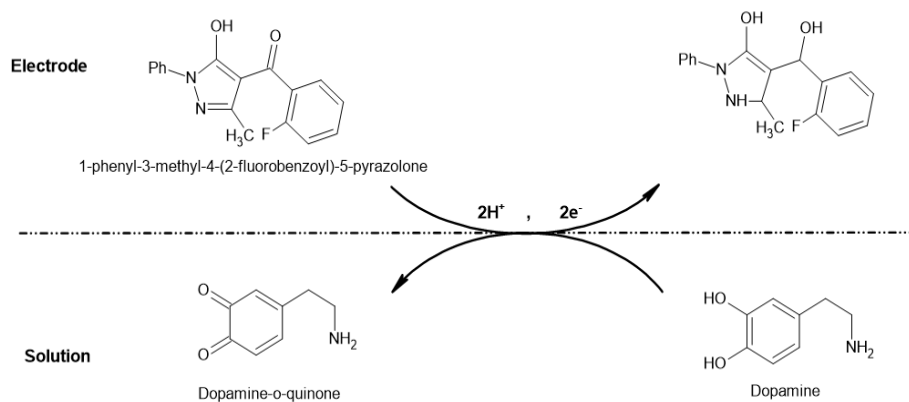
The impact of pH on peak potential (E) of DOP was also investigated. As been observed, the DOP oxidation peak potential shifted negatively with the increment of pH buffer indicated involvement of protons in the DOP oxidation, and the dependence of peak potential of DOP towards pH displayed linear relation which can be expressed as $E = -51.292 \text{ pH} + 581.489$ ($R^2 = 0.9973$). The slope value of 51.3 mV pH^{-1} over the pH range (6.0-8.4) was close to the Nernstian

theoretical slope value of -59 mV proposing the same number of electrons and protons involved in the DOP reaction [23]. Supporting this, the number of protons that involved in the electro-oxidation reaction of HPMoFBP/MWCNT was calculated using the following Nernst relation, Eq. (2).

$$B = -2.3025 m R T / n F \quad (2)$$

where B is the slope of linear regression equation, m is the number of protons that participated in the DOP oxidation reaction, n is the number of electrons participating in the DOP oxidation reaction and other terms (R , T and F) represents their standard physical values. The determined value for the number of protons was found to be $1.7 \approx 2$. This indicates the DOP oxidation is a two-electron process.

Scheme 1 illustrates the proposed mechanism for the oxidation reaction of DOP at the HPMoFBP/MWCNT paste electrode. In a solution, DOP was oxidized electrochemically to produce dopamine-o-quinone by releasing two protons and electrons while in an electrode surface, the HPMoFBP accepting those protons and electrons.



Scheme 1. Illustration of the proposed reaction mechanism at the HPMoFBP/MWCNT paste electrode and DOP solution.

Chronocoulometry study

A series of stepped polarizations is used in chronocoulometry to measure the charge generated from reactants adsorbed at an electrode interface [24]. Thus, double potentials step chronocoulometry experiment has been implemented in determine the electrochemical effective area and saturation adsorption capacity of the HPMoFBP/MWCNT and bare MWCNT. The study employed 4.0×10^{-3} M $K_4[Fe(CN)_6]$ containing 1.0×10^{-1} M KCl. The calculation was given by Anson's equation, Eq. (3).

$$Q(t) = 2 n F A C D^{1/2} t^{1/2} / \pi^{1/2} + Q_{dl} + Q_{ads} \quad (3)$$

where D is the $K_4[Fe(CN)_6]$ standard diffusion coefficient, Q_{dl} is the double layer charge, F is the Faraday's constant (96485 C), Q_{ads} is the Faradic charge, n is the number of electron, and C is the concentration of the substrate (mol cm^{-3}).

When Q was plotted against time, $t^{1/2}$, it revealed a linear connection with the following equation, Eq. (4):

$$Q = 8.924 \times 10^{-5} t^{1/2} - 4.344 \times 10^{-5},$$

$$Q = 1.312 \times 10^{-3} t^{1/2} - 1.310 \times 10^{-3}. \quad (4)$$

The slope of the linear connection between Q and $t^{1/2}$ was used to obtain the effective surface area (A). According to the slopes of $8.924 \times 10^{-5} \text{ C s}^{-1/2}$ (bare MWCNT), and $1.312 \times 10^{-3} \text{ C s}^{-1/2}$ (HPMoFBP/MWCNT), the effective surface area (A) for the bare MWCNT and HPMoFBP/MWCNT were 1.17×10^{-1} and 1.71 cm^2 , respectively suggesting the modification of MWCNT with HPMoFBP improved the effective surface area of the electrode, which further enhanced the current response (Figure 5A).

The diffusion coefficient (D) and Faradic charge (Q_{ads}) of DOP at the HPMoFBP/MWCNT could be determined by double potentials step chronocoulometry experiment towards $1.0 \times 10^{-4} \text{ M}$ DOP in $1.0 \times 10^{-1} \text{ M}$ PBS (pH 8.0). From the plot of charge (Q) vs. square root of time ($t^{1/2}$), the slope and intercept (Q_{ads}) were found to be $3.261 \times 10^{-3} \text{ C s}^{-1/2}$ and $-2.881 \times 10^{-3} \text{ C}$, respectively as can be showed in Figure 5B. As a result, D was calculated to be $7.67 \times 10^{-3} \text{ cm}^2 \text{ s}^{-1}$. The adsorption capacity (Γ) of the HPMoFBP/MWCNT can be measured based on the Eq. (5).

$$Q_{ads} = n F A \Gamma \quad (5)$$

Based on the data obtained, the Γ value of the HPMoFBP/MWCNT has been calculated as $8.73 \times 10^{-9} \text{ mol cm}^{-2}$ which proposing good adsorption capacity for DOP detection.

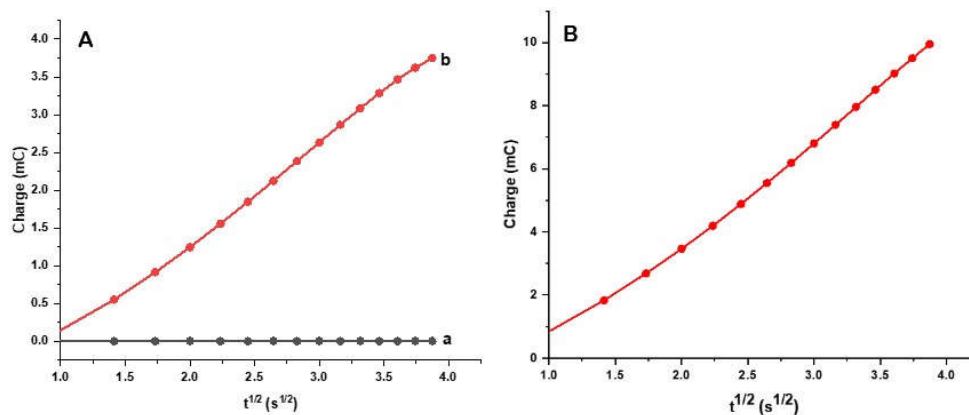


Figure 5. (A) Chronocoulograms of (a) bare MWCNT and (b) HPMoFBP/MWCNT paste electrode in $4 \times 10^{-3} \text{ M}$ $\text{K}_4[\text{Fe}(\text{CN})_6]$ in $1.0 \times 10^{-1} \text{ M}$ KCl, and (B) Chronocoulograms of HPMoFBP/MWCNT paste electrode in $1.0 \times 10^{-4} \text{ M}$ of DOP solution ($1.0 \times 10^{-1} \text{ M}$ PBS, pH 8.0)

Scan rate effect on DOP peak currents

To investigate the reaction kinetics of HPMoFBP/MWCNT, the scan rate effect on the DOP peak current at the HPMoFBP/MWCNT paste electrode surface was studied in $1.0 \times 10^{-3} \text{ M}$ DOP ($1.0 \times 10^{-1} \text{ M}$, PBS pH 8.0). According to the Randles-Sevcik equation, the scan rate is proportionate to the peak current. DOP peak currents arose gradually with the increment of scan rate from 40 to 400 mV s^{-1} and shifted positively for the anodic peak current while negatively for the cathodic peak current, indicating kinetic limitation in the reaction as displayed in the Figure 6A. To

determine the kind of mechanism occurred in the electrode, the graph of peak currents versus scan rate was plotted as can be observed in Figure 6B and it displays straight line with the linear regression equations, current (I_{pc}) = $-0.0333v + 0.2565$ and Curren (I_{pa}) = $0.0311v + 1.7115$ illustrating an adsorption-controlled process. The correlation coefficients were found to be 0.9866 and 0.9906, respectively. To validate the occurred process, a log plot between peak currents and scan rate has been constructed as can be seen in Figure 6C. A good linear relationship with the equation of $\log I_{pa} = 0.71 \log v - 0.70$ ($R^2 = 0.998$) has been achieved. The obtained slope value which is 0.71 (theoretical value, 1.0) further confirmed that the adsorption process has been occurred at the surface of the electrode [22].

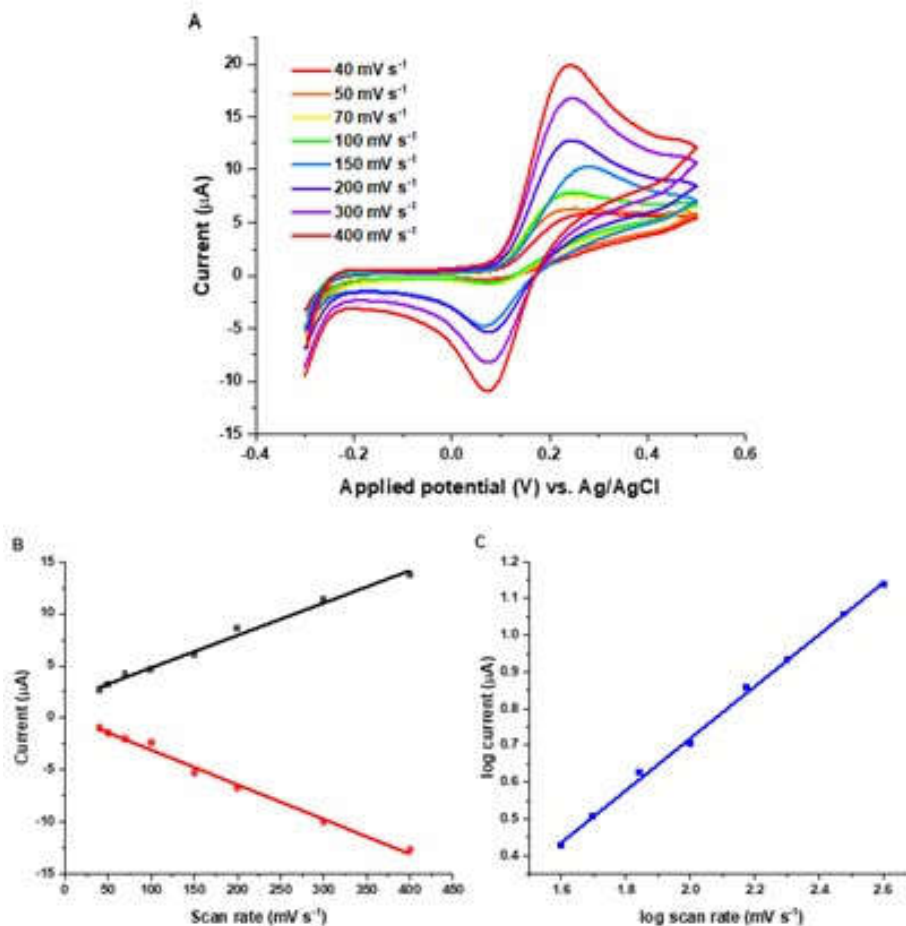


Figure 6. CV of 1×10^{-3} M DOP at the HPMoFBP/MWCNT in 1.0×10^{-1} M PBS, pH 8.0 at (A) scan rates of 40, 50, 70, 100, 150, 200, 300, and 400 mV s^{-1} and (B) plot of peak currents versus scan rate, and (C) plot of log peak currents versus log scan rate.

Calibration curve and limit of detection

Under the specific conditions of SWV parameters, the electrocatalytic oxidation of DOP has been studied on the HPMoFBP/MWCNT using varies concentration. The peak current (μ A) plot

against DOP concentration as exhibited in the Figure 7 shows linear relationship in the DOP working range from 1 to 1000 μM with linear regression equation as $\text{Current } (\mu\text{A}) = 0.082 [\text{DOP}] - 1.1811$ ($R^2 = 0.9905$). The limit of detection (LOD) was estimated to be 1.0×10^{-7} M where the calculated value been obtained by using Eq. (6).

$$\text{LOD} = 3\sigma/m \quad (6)$$

m is the slope obtained from the calibration curve and σ is the relative standard deviation of its intercept.

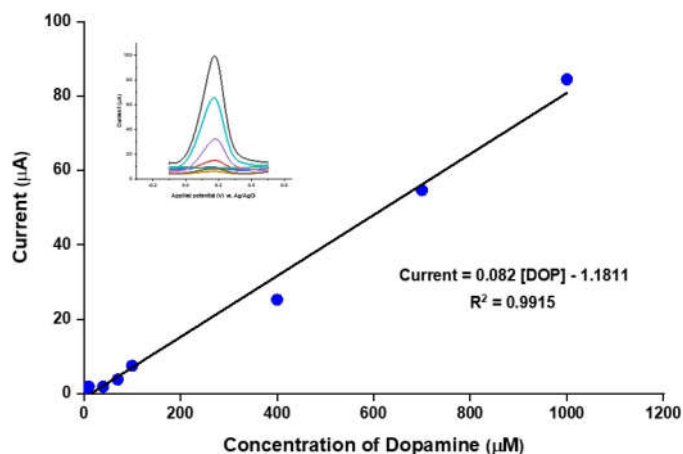


Figure 7. DOP calibration curve. Inset shows the SWV responses to the DOP different concentrations.

Table 1 shows the high sensitivity of the HPMoFBP/MWCNT paste electrode compared to those obtained for several other electrodes using different electroanalytical techniques. The obtained results shows that the proposed sensor exhibits quite good sensitivity and suggested could be used for the DOP determination in biological analytes and environmental.

Table 1. Comparison of analytical performance of the fabricated electrodes for the DOP detection.

Electrode	Technique	Calibration curve (M)	LOD (M)	Ref.
CoFe ₂ O ₄ /GP	DPV	$3.0 \times 10^{-6} - 1.8 \times 10^{-4}$	3.5×10^{-7}	[23]
MnFe ₂ O ₄ /GP	DPV	$5.0 \times 10^{-6} - 2.0 \times 10^{-4}$	4.0×10^{-7}	[23]
PPy/rGO/carbon fibre	DPV	$0 - 5.0 \times 10^{-4}$	6.0×10^{-6}	[7]
COF-NH ₂ -MWCNT/Au /GCE	DPV	$4.0 \times 10^{-7} - 1.08 \times 10^{-4}$	2.1×10^{-7}	[24]
Au/NF/CD/AuNPs	DPV	$5.0 \times 10^{-8} - 2.0 \times 10^{-7}$	6.0×10^{-10}	[20]
Zn/Al-LDH-CP/MWCNT/CPE	SWV	$7.0 \times 10^{-6} - 5.0 \times 10^{-4}$	1.7×10^{-7}	[25]
Ni-Zr/MSN/GCE	DPV	$3.0 \times 10^{-7} - 1.0 \times 10^{-4}$	1.3×10^{-7}	[26]
EDTA-MWCNT/AuNPs	CV	$1.0 \times 10^{-8} - 6.0 \times 10^{-6}$	3.0×10^{-9}	[27]
UiO-66-NH ₂ /CNTs/GCE	DPV	$3.0 \times 10^{-8} - 2.0 \times 10^{-6}$	1.5×10^{-8}	[28]
ZLH-SDS-I/MWCNT/CPE	SWV	$1.0 \times 10^{-6} - 3.0 \times 10^{-4}$	4.3×10^{-7}	[29]
PNA/AuNPs/GCE	CV	$5.0 \times 10^{-6} - 3.5 \times 10^{-5}$	6.11×10^{-7}	[30]
HPMoFBP/MWCNT/CPE	SWV	$1.0 \times 10^{-6} - 1.0 \times 10^{-3}$	1.0×10^{-7}	This work

Interference study of the HPMoFBP/MWCNT

The interference from some possible coexisting interfering species such as potassium chloride, magnesium chloride, sodium chloride, lysine, potassium nitrate, and sodium sulphate has been investigated by evaluating differences in the oxidation peak current value of 1.0×10^{-4} M DOP in 1.0×10^{-1} M PBS (pH 8.0). Tolerance limit of below than 10% has been selected as a maximum concentration of foreign substances that caused relative error on DOP detection. This study found that all substances (till 25-fold excess) did not interfere the DOP detection, thus proposing that the HPMoFBP/MWCNT possesses excellent selectivity.

Reproducibility, stability, and repeatability

The electrodes' performance in terms of reproducibility, stability, and repeatability are all crucial characteristics. Those electrodes have been investigated by measuring the responses of the HPMoFBP/MWCNT in the presence of 1.0×10^{-4} M DOP in 1.0×10^{-1} M PBS (pH 8.0). The reproducibility was tested using four identically produced electrodes, and the relative standard deviation (RSD) was determined to be 3.40%, indicating that the modified electrode showed good reproducibility. In addition, ten successive measurements were taken with the same modified electrode, and the repeatability was found to be 3.34% when the RSD was calculated. The stability of the prepared modified sensor was determined by observing the current response towards dopamine oxidation after 14 days of operation. After 35 times of measurement, the current was observed to preserve around 90% of its original response, proposing good stability of HPMoFBP/MWCNT. These results show that the HPMoFBP/MWCNT was stable and expected to be used the presence of DOP in real samples [18].

Real sample analysis

Under optimum experimental conditions, the potential of HPMoFBP/MWCNT as sensor in detecting the DOP content in dopamine hydrochloride injection was studied by SWV. The calibration curve method has been used, and the obtained results are shown in Table 2. The injection was diluted prior to use. The results showed good percentage of recovery with the range of 91 to 98%, thus suggesting the HPMoFBP/MWCNT could be efficiently applied for DOP detection.

Table 2. DOP detection in Dopamine Hydrochloride Injection (n = 3).

Sample	DOP added (M)	DOP found (M)	Recovery (%)	RSD (%)
Dopamine hydrochloride injection	1.5×10^{-4}	1.47×10^{-4}	98	0.19
	2.5×10^{-4}	2.28×10^{-4}	91	0.38

CONCLUSION

A highly sensitive, cost effective, and simple sensing material HPMoFBP/MWCNT was proposed for the detection of DOP with low LOD. The modified electrode expressed good electrocatalytic activity for the electrochemical detection of DOP including better sensitivity and selectivity of the modified electrode towards DOP oxidation at pH 8.0. Therefore, the modified electrode may have great application potential in the sensing field.

ACKNOWLEDGEMENT

The authors would like to express their thankfulness to the Sultan Idris Education University (UPSI) for the Rising Star Grant (Grant Number: 2019-0120-103-01) in funding the research.

REFERENCES

1. Donati, E.; Aturki, Z. *Capillary Electrophoresis in Food Analysis*, 1st ed., Bentham Science Publishers Pte. Ltd: Singapore; **2022**; p 450.
2. Karthik, V.; Selvakumar, P.; Senthil Kumar, P.; Satheeskumar, V.; Godwin Vijaysunder, M.; Hariharan, S.; Antony, K. Recent advances in electrochemical sensor developments for detecting emerging pollutant in water environment. *Chemosphere* **2022**, 304, 135331.
3. Lu, L.; Lin, J.; Zhang, K.; Gao, D.; Wang, D. Molecularly imprinted polymers based on magnetic metal-organic frameworks for surface-assisted laser desorption/ionization time-of-flight mass spectrometry analysis and simultaneous luteolin enrichment. *J. Chromatogr. A* **2022**, 1678, 463377.
4. Qi, H.; Zhang, C. Organic nanoparticles for electrogenerated chemiluminescence assay. *Curr. Opin. Electrochem.* **2022**, 34, 101023.
5. Salerno, T.M.G.; Coppolino, C.; Donato, P.; Mondello, L. The online coupling of liquid chromatography to Fourier transform infrared spectroscopy using a solute-deposition interface: A proof of concept. *Anal. Bioanal. Chem.* **2022**, 414, 703-712.
6. Moallem, Q.A.; Beitollahi, H. Electrochemical sensor for simultaneous detection of dopamine and uric acid based on a carbon paste electrode modified with nanostructured Cu-based metal-organic frameworks. *Microchem. J.* **2022**, 177, 107261.
7. Sriprasertsuk, S.; Zhang, S.; Wallace, G.; Chen, J.; Varcoe, J.R.; Crean, C. Reduced graphene oxide carbon yarn electrodes for drug sensing. *Front. Sens.* **2021**, 2, 719161.
8. Rejithamol, R.; Beena, S. Carbon paste electrochemical sensors for the detection of neurotransmitters. *Front. Sens.* **2022**, 3, 901628.
9. Maaroo, Y.T.; Mahmoud, K.M. Silver nanoparticle-modified graphite pencil electrode for sensitive electrochemical detection of chloride ions in pharmaceutical formulations. *Bull. Chem. Soc. Ethiop.* **2023**, 37, 491-503.
10. Fredj, Z.; Sawan, M. Advanced nanomaterials-based electrochemical biosensors for catecholamines detection: Challenges and trends. *Biosensors* **2023**, 13, 211.
11. Abedul, M.T.F. *Laboratory Methods in Dynamic Electroanalysis*, 1st ed., Elsevier: Amsterdam; **2019**; p 2-3.
12. Franco, R.; Reyes-Resina, I.; Navarro, G. Dopamine in health and disease: Much more than a neurotransmitter. *Biomedicines* **2021**, 9, 109.
13. Masood, T.; Asad, M.; Riaz, S.; Akhtar, N.; Hayat, A.; Shenashen, M.A.; Rahman, M.M. Non-enzymatic electrochemical sensing of dopamine from COVID-19 quarantine person. *Mater. Chem. Phys.* **2022**, 289, 126451.
14. Šik Novak, K.; Bogataj Jontez, N.; Kenig, S.; Hladnik, M.; Baruca Arbeiter, A.; Bandelj, D.; Jenko Pražnikar, Z. The effect of COVID-19 lockdown on mental health, gut microbiota composition and serum cortisol levels. *Stress* **2022**, 25, 246-257.
15. Lakard, S.; Pavel, I.A.; Lakard, B. Electrochemical biosensing of dopamine neurotransmitter: A review. *Biosensors* **2021**, 11, 179.
16. Asif, M.; Imran, M.; Husain, A. Approaches for chemical synthesis and diverse pharmacological significance of pyrazolone derivatives: a review. *J. Chil. Chem. Soc.* **2021**, 66, 5149-5163.
17. Yusri, W.T.; Yulkifli, Y.; Alizar, A.; Isa, I.M. Synthesis and characterization of HPMpFBP using Raman spectroscopy, nuclear magnetic resonance (NMR) spectroscopy, and FTIR. *J. Ilmu Fisika* **2021**, 13, 109-117.
18. Zainul, R.; Isa, I.M.; Yazid, N.A.M.; Hashim, N.; Mohd Sharif, S. N.; Amir, Y. Enhanced electrochemical sensor for electrocatalytic glucose analysis in orange juices and milk by the integration of the electron-withdrawing substituents on graphene/glassy carbon electrode. *J. Anal. Methods Chem.* **2022**, 2022, 5029036.

19. Hua, Z.; Qin, Q.; Bai, X.; Wang, C.; Huang, X. β -Cyclodextrin inclusion complex as the immobilization matrix for laccase in the fabrication of a biosensor for dopamine determination. *Sens. Actuators B Chem.* **2015**, *220*, 1169-1177.
20. Atta, N.F.; Galal, A.; El-Said, D.M. Novel design of a layered electrochemical dopamine sensor in real samples based on gold nanoparticles/ β -cyclodextrin/nafion-modified gold electrode. *ACS Omega* **2019**, *4*, 17947-17955.
21. Pomeroy, E.D.; Maza, W.A.; Steinhurst, D.A.; Owrutsky, J.C.; Walker, R.A. Electrochemical sulfur oxidation in solid oxide fuel cells studied by near infrared thermal imaging and chronocoulometry. *J. Electrochem. Soc.* **2020**, *167*, 164511.
22. Laviron, E.; Roullier, L.; Degrand, C. A multilayer model for the study of space distributed redox modified electrodes: Part II. Theory and application of linear potential sweep voltammetry for a simple reaction. *J. Electroanal. Chem. Interfacial Electrochem.* **1980**, *112*, 11-23.
23. Kumar, Y.; Pramanik, P.; Das, D.K. Electrochemical detection of paracetamol and dopamine molecules using nano-particles of cobalt ferrite and manganese ferrite modified with graphite. *Heliyon* **2019**, *5*, e02031.
24. Guan, Q.; Guo, H.; Xue, R.; Wang, M.; Zhao, X.; Fan, T.; Yang, W. Electrochemical sensor based on covalent organic frameworks-MWCNT-NH₂/AuNPs for simultaneous detection of dopamine and uric acid. *J. Electroanal. Chem.* **2021**, *880*, 114932.
25. Abd Azis, N.; Isa, I.M.; Hashim, N.; Ahmad, M.S.; Yazid, N.A.M.; Mukdasai, S. Synergistic effect of zinc/aluminium-layered double hydroxide-clopyralid carbon nanotubes paste electrode in the electrochemical response of dopamine, acetaminophen, and bisphenol A. *Int. J. Electrochem. Sci.* **2020**, *15*, 9088-9107.
26. Roduan, M.R.A.M.; Saidin, M.I.; Sidik, S.M.; Abdullah, J.; Isa, I.M.; Hashim, N.; Ahmad, M.S.; Yazid, S.N.A.M.; Bahari, A. A. New modified mesoporous silica nanoparticles with bimetallic Ni-Zr for electroanalytical detection of dopamine. *J. Electrochem. Sci. Eng.* **2022**, *12*, 463-474.
27. Tang, C.R.; Tian, G.; Wang, Y.J.; Su, Z.H.; Li, C.X.; Lin, B.G.; Huang, H.W.; Yu, X.Y.; Li, X.F.; Long, Y.F.; Zeng, Y.L. Selective response of dopamine in the presence of ascorbic acid and uric acid at gold nanoparticles and multi-walled carbon nanotubes grafted with ethylene diamine tetraacetic acid modified electrode. *Bull. Chem. Soc. Ethiop.* **2009**, *23*, 317-326.
28. Li, Y.; Shen, Y.; Zhang, Y.; Zeng, T.; Wan, Q.; Lai, G.; Yang, N. A UiO-66-NH₂/carbon nanotube nanocomposite for simultaneous sensing of dopamine and acetaminophen. *Anal. Chim. Acta* **2021**, *1158*, 338419.
29. Ahmad, M.S.; Isa, I.M.; Hashim, N.; Saidin, M.I.; Suyanta, S.; Zainul, R.; Mukdasar, S. Zinc layered hydroxide-sodium dodecyl sulphate-isoprocarb modified multiwalled carbon nanotubes as sensor for electrochemical determination of dopamine in alkaline medium. *Int. J. Electrochem. Sci.* **2019**, *14*, 9080-9091.
30. Olana, B.N.; Kitte, S.A.; Geletu, A.K.; Soreta, T.R. Selective electrochemical determination of dopamine at p-nitroaniline film-hole modified glassy carbon electrodes. *Bull. Chem. Soc. Ethiop.* **2017**, *31*, 361-372.